High resolution phoswich gamma-ray imager utilizing monolithic MPPC arrays with submillimeter pixelized crystals

2013 JINST 8 P05022

(http://iopscience.iop.org/1748-0221/8/05/P05022)

J inst

PUBLISHED BY IOP PUBLISHING FOR SISSA MEDIALAB

RECEIVED: *March 18, 2013*
ACCEPTED: *May 2, 2013*
PUBLISHED: *May 28, 2013*

High resolution phoswich gamma-ray imager utilizing monolithic MPPC arrays with submillimeter pixelized crystals

T. Kato,[a,1] J. Kataoka,[a] T. Nakamori,[a] A. Kishimoto,[a] S. Yamamoto,[b] K. Sato,[c] Y. Ishikawa,[c] K. Yamamura,[c] N. Kawabata,[c] H. Ikeda[d] and K. Kamada[e]

[a]*Research Institute for Science and Engineering, Waseda University, Shinjuku, Tokyo 169-8555, Japan*

[b]*Nagoya University Graduate School of Medicine, 1-1-20, Daikominami, Higashi-ku, Nagoya-shi, Aichi 461-8673, Japan*

[c]*Hamamatsu Photonics, K.K., 1126-1, Ichino-cho, Higashi-ku, Hamamatsu-shi, Shizuoka 435-8558, Japan*

[d]*ISAS/JAXA, 3-1-1, Yoshinodai, Chuo-ku, Sagamihara-shi, Kanagawa, 252-5210, Japan*

[e]*Materials Research Laboratory, Furukawa Co., Ltd., 1-25-13, Kannondai, Tsukuba, Ibaraki, 305-0856, Japan*

E-mail: katou.frme.8180@asagi.waseda.jp

ABSTRACT: We report the development of a high spatial resolution tweezers-type coincidence gamma-ray camera for medical imaging. This application consists of large-area monolithic Multi-Pixel Photon Counters (MPPCs) and submillimeter pixelized scintillator matrices. The MPPC array has 4×4 channels with a three-side buttable, very compact package. For typical operational gain of 7.5×10^5 at $+20\,^\circ$C, gain fluctuation over the entire MPPC device is only $\pm 5.6\%$, and dark count rates (as measured at the 1 p.e. level) amount to ≤ 400 kcps per channel. We selected Ce-doped $(Lu,Y)_2(SiO_4)O$ (Ce:LYSO) and a brand-new scintillator, Ce-doped $Gd_3Al_2Ga_3O_{12}$ (Ce:GAGG) due to their high light yield and density. To improve the spatial resolution, these scintillators were fabricated into 15×15 matrices of 0.5×0.5 mm^2 pixels. The Ce:LYSO and Ce:GAGG scintillator matrices were assembled into phosphor sandwich (phoswich) detectors, and then coupled to the MPPC array along with an acrylic light guide measuring 1 mm thick, and with summing operational amplifiers that compile the signals into four position-encoded analog outputs being used for signal readout. Spatial resolution of 1.1 mm was achieved with the coincidence imaging system using a ^{22}Na point source. These results suggest that the gamma-ray imagers offer excellent potential for applications in high spatial medical imaging.

KEYWORDS: Intra-operative probes; Gamma camera, SPECT, PET PET/CT, coronary CT angiography (CTA); Photon detectors for UV, visible and IR photons (solid-state) (PIN diodes, APDs, Si-PMTs, G-APDs, CCDs, EBCCDs, EMCCDs etc)

[1]Corresponding author.

doi:10.1088/1748-0221/8/05/P05022

2013 JINST 8 P05022

Contents

1 Introduction

Positron emission tomography (PET) imaging is a promising method for investigating pathological phenomena, detecting cancers in its early stages and diagnosing disease such as Alzheimer's [1]. Many advantageous aspects of PET combined with Magnetic Resonance Imaging (MRI) have being proposed (MRI-PET), and with prototypes now being tested as MRI produces an excellent soft-tissue contrast and anatomical detail without additional radiation [2–4]. For a long time, a Photo-Multiplier Tube (PMT) has been used as a photodetector of PET scanners because they have high gain, good timing property, temperature stability and low cost. However, PMTs have several disadvanteges such as sensitivity to magnetic field which disturbs their use within the high magnetic field of Magnetic Resonance Imaging (MRI). Moreover the large-size PMT-base PET not only complicates use in narrow MRI tunnels but also limits the spatial resolution far from the theoretical limits of PET resolution. Currently, semiconductor photodetector-based high resolution PET scanners have being proposed and tested as semiconductor photodector is compact and insensitive to maginetic field.

On the other hand, gamma camera for positron-guide surgery have been proposed and attempted [5–7]. This application aimed to intraoperatively detect the radiation emission (β or/and annihilation gamma-ray) from the ^{18}F-fluorodeoxyglucose (FDG). It can not only detect the positions of cancers but also make sure that excised segment contain cancers, so that cancers can be completly removed from a patient. The coincidence method is more suitable for this application as it can reduce the gamma background effectively [8]. Ref. [9] proposed the tweezers type coincidence camera, which consist of two detectors attached to the tips of tweezers. The coincidence

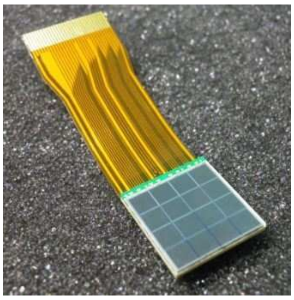

Figure 1. Photo of the 4×4 MPPC array developed in this paper.

camera has high potential for detecting ^{18}F source, but the spatial resolution is few mm and its large size make difficult to use in clinical practice. In order to improve the spatial resolution and minimize the application, the compact semiconductor phodoetector is suitable, as is the case for PET scanners.

Multi-Pixel Photon Counter (MPPC), also known as a Silicon Photo-Multiplier (SiPM), is a high performance semiconductor photodetector consisting of multiple Geiger-mode avalanche photodiode (APD) pixels. The MPPC has many advantages such as compactness and insensitivity to magnetic fields. In addition, it is operated in Geiger-mode, meaning its gain may be almost comparable to that of PMTs at up to the $10^5 \sim 10^6$ level, resulting in good signal-to-noise (S/N) ratio and excellent timing property [10]. These great advantages make the MPPC an ideal photosensor for PET as well as for the coincidence gamma camera for positron-guide surgery.

We previously developed and tested a monolithic, three-side buttable 4×4 MPPC array with submillimeter pixelized Ce-doped $(Lu,Y)_2(SiO_4)O$ (Ce:LYSO) and Ce-doped $Gd_3Al_2Ga_3O_{12}$ (Ce:GAGG) scintillator matrices [11]. In the position histograms, each scintillator pixel is clearly resolved, suggesting the possibility of its use as a compact and submillimeter high resolution gamma-ray imaging application. Therefore, we fabricated and a tested tweezers type coincidence gamma-ray imager using the MPPC array and the submillimeter pixelized scintillators. Furthermore, we evaluated a spatial resolution of prototype gantry for a PET scanner.

This paper is organised as follows. In section 2, we present the basic characters of the MPPC array, and the Ce:LYSO and Ce:GAGG scintillators. In section 3, configuration and performance of the tweezer type coincidence gamma-ray imager are given. In section 4, we present the experimental measurement of the prototype gantry for a PET scanner. The final conclusions are presented in section 5.

2 MPPC and scintillators

2.1 4×4 monolithic MPPC array

Figure 1 shows a picture of the monolithic 4×4 MPPC array [12] developed in this paper. The MPPC array was designed and developed for future applications in nuclear medicine (such as PET scanners) by Hamamatsu Photonics K.K.. Each channel has a photosensitive area of 3×3 mm^2 containing 60×60 Geiger mode avalanche photodiodes (APDs) arranged with a pitch of 50 μm. The gap between each channel is only 0.2 mm thanks to the monolithic structure. The MPPC array

2013 JINST 8 P05022

Table 1. Specification of the 4 × 4 MPPC array at + 25 deg.

Parameters	Specification
Number of elements [ch]	4×4
Effective active area / channel [mm]	3×3
Pixel size of a Geiger-mode APD [μm]	50
Number of pixels / channel	3600
Typical photon detection efficiency[1] (λ=440 nm) [%]	50
Typical dark count rates / channel [kcps]	≤ 400
Terminal capacitance / channel [pF]	320
Gain (at operation voltage)	7.5×10^5

[1]: Including cross-talk and after-pulse contributions.

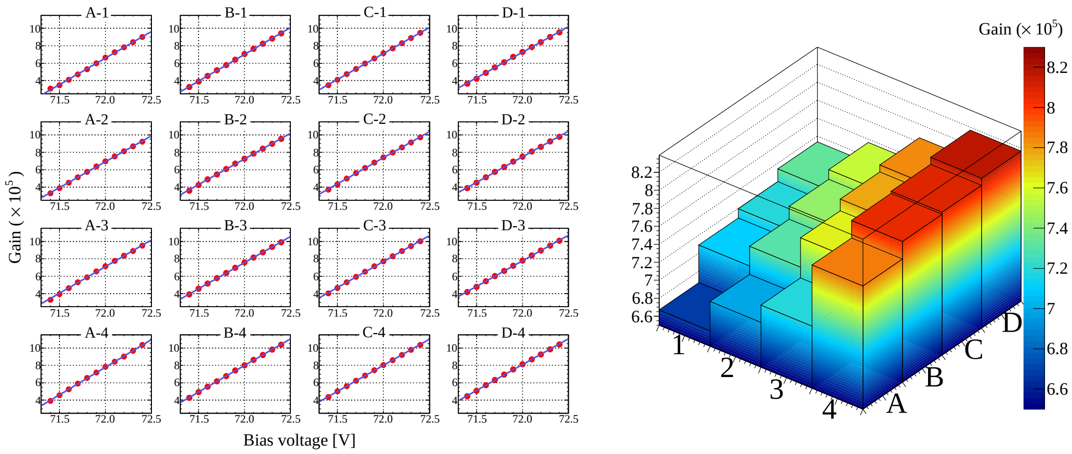

Figure 2. *Left*: gain variation as a function of bias voltage for all pixels from 71.4 to 72.4 V, measured at +20 degrees. *Right:* gain distribution at the operation voltage of 72.01 V

is placed on a surface-mounted package measuring 14.3 by 13.6 mm, and fabricated into a three-side buttable structure, that is, the distance from the photosensitive area to the edge of the package is only 500 μm. An excellent gain uniformity ($\pm$ 5.6%) (figure 2) and very low dark count rates ($\leq$400 kcp, due to the 1 p.e. level) have been achieved at an averaged gain of 7.5×10^5, measured at +20 degrees. Table 1 lists the other basic characteristics of the MPPC array.

Also, the energy and time resolutions were obtained as 11.5 ± 0.5% (FWHM at 662 keV photoelectric peak) and 493 ± 22 ps (FWHM), respectively when the MPPC array were optically coupled with a Ce:LYSO scintillator [11].

2.2 Scintillators

To fabricate gamma-ray imaging applications, we selected Ce:LYSO and Ce:GAGG scintillators. Ce:LYSO, which is one of the most popular scintillator at present in medical imaging, has features such as high light yield (75% of Tl:NaI), short scintillation decay time (40 nsec) and high density (7.4 g/cm^3) greater than $Bi_{12}Ge_3O_{20}$ (BGO) (7.1 g/cm^3) [13]. However, Ce:LYSO contains a considerable amount of self radiation emitted from ^{176}Lu. Alternatively, a brand-new scintillator, Ce:GAGG also have very high light yield and short scintillator decay time, and it is noteworthy that

2013 JINST 8 P05022

Table 2. Basic characteristics of the Ce:LYSO and Ce:GGAG scintillators.

	Ce:LYSO	Ce:GGAG
Density [g/cm^3]	7.10	6.63
Light yield [photons/MeV]	25,000	46,000
Decay time [nsec]	40	88(91%) and 258(9%)
Peak wavelength [nm]	420	520

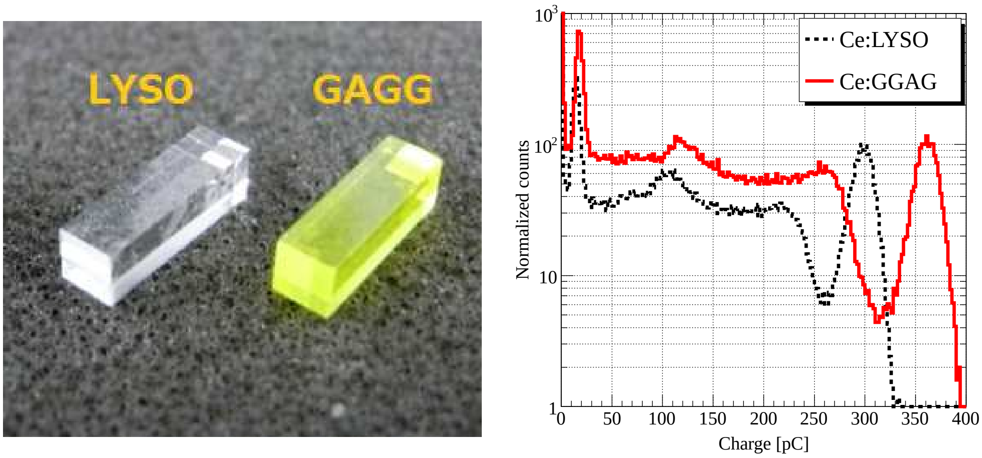

Figure 3. *Left*: photo of the $3 \times 3 \times 10$ mm^3 Ce:LYSO and the Ce:GAGG scintillators. *Right*: energy spectra of ^{137}Cs source. Red line and dashed black line represent the Ce:GAGG and Ce:LYSO, respectively.

Ce:GAGG has no self radiation [14]. Table 2 lists the other basic characteristics of the Ce:LYSO and the Ce:GAGG scintillators.

Figure 3 (*right*) shows ^{137}Cs spectra obtained by using a $3 \times 3 \times 10$ mm^3 Ce:LYSO and Ce:GAGG (figure 3 ($left$)) crystals with a 50 μm-type 3×3 mm^2 MPPC (Hamamatsu:S10362-33-050C), measured at +20 degrees. The MPPC was operated at the gain of 7.5×10^5. Typically, MPPCs are most sensitive within the range of 350-500 nm [15]. In this sense, a emission of the Ce:GAGG, peaking at 520 nm is not favorable, but the output signal from the MPPC with the Ce:GAGG was about 21% larger than that of the Ce:LYSO due to the high light yield of Ce:GAGG. The energy resolution for the 662 keV photoelectric peak were 9.9% and 7.9% for the Ce:LYSO and the Ce:GAGG after linearity correction [16], respectively. Their high light yield should provide the better energy resolution, and moreover, good spatial resolution when they are fabricated in small pixels and read out by a charge division resistor network [17].

3 Tweezers type imaging system

3.1 Setup

The tweezers type imaging system has two phosphor sandwich (phoswich) gamma-ray detector blocks consisting of the MPPC arrays, Ce:LYSO and Ce:GAGG scintillator matrices. These scin-

2013 JINST 8 P05022

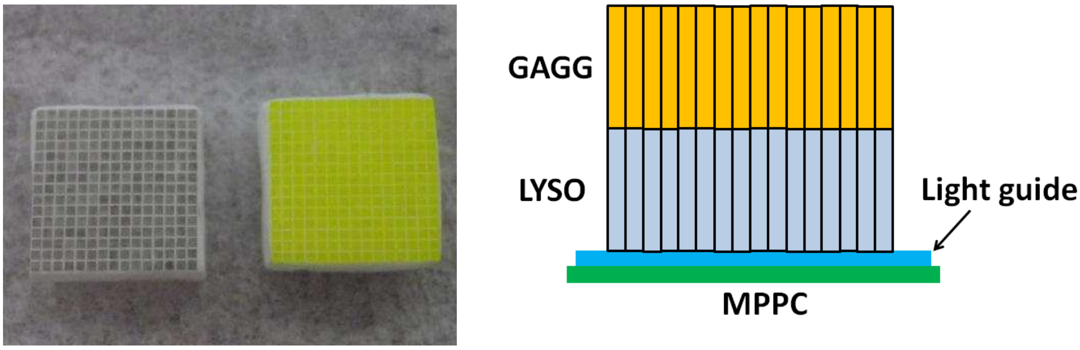

Figure 4. *Left*: photos of the 15×15 of 0.5×0.5 mm^2 Ce:LYSO (left side) and Ce:GAGG (right side) matrices. *Right*: configuration of the two-layer phoswich gamma-ray detector block. The MPPC array, the acrylic light guide, the Ce:LYSO and the Ce:GAGG scintillator matrices are optically coupled each other.

Figure 5. Photo of the tweezer mounted a pair of MPPC arrays coupled with the 0.5×0.5 mm^2 Ce:LYSO and Ce:GAGG scintillator matrices.

tillator matrices are composed of 15×15 matrices of 0.5×0.5 mm^2 pixels optically separated by $BaSO_4$ layer 0.1 mm thick (figure 4 ($left$)). The total size of the scintillator matrices are $9.7 \times 9.7 \times 5$ mm^3, and the configurations of each matrix is completely matched. The Ce:LYSO matrix was coupled to the MPPC array with the acrylic light guide 1 mm thick, which distributes scintillator photons across multiple MPPC array channels, and the Ce:GAGG matrix was coupled to the other side of the Ce:LYSO matrix (figure 4 (*right*)). They are copuled each other by optical grease. The detector block is capable of two-layer Depth of Interaction (DoI) measurement by identifying in which scintillator matrices the event occured. Two detector blocks were then attached on acrylic tongs, and form a tweezers type coincidence gamma-ray imager (figure 5).

Output signals from the MPPC arrays were fed into a coincidence DAQ system developed by ESPEC TECHNO CORP. after compiled four position-encoded analog outputs (x direction; X_+ and X_-, y direction; Y_+ and Y_-) by the summing operational amplifiers [17, 18]. The compiled signals were digitized by a 100 M samples/s ADC (AD9218 BST-105), and then, processed by field-programmable gate arrays (FPGAs). When the digital signals were over the threshold of digital comparator, the signals are integrated with two different integration time (130 ns and 320 ns). The positional distributions were calculated by the Anger-logic; $x = (X_+/(X_+ + X_-))$ and $y = (Y_+/(Y_+ + Y_-))$, and the energy was delivered from the sum of four signals. If the timing signals

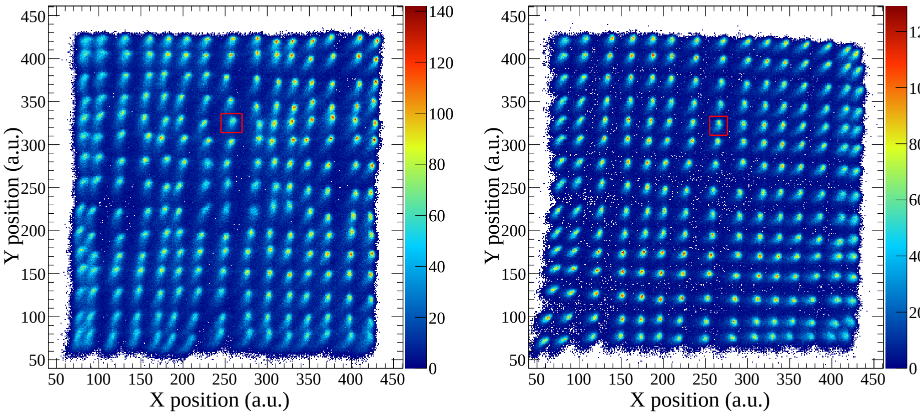

Figure 6. Flood images of 15×15 of 0.5×0.5 mm^2 Ce:LYSO (*Left*) and Ce:GAGG (*Right*) scintillator matrices with a ^{137}Cs source.

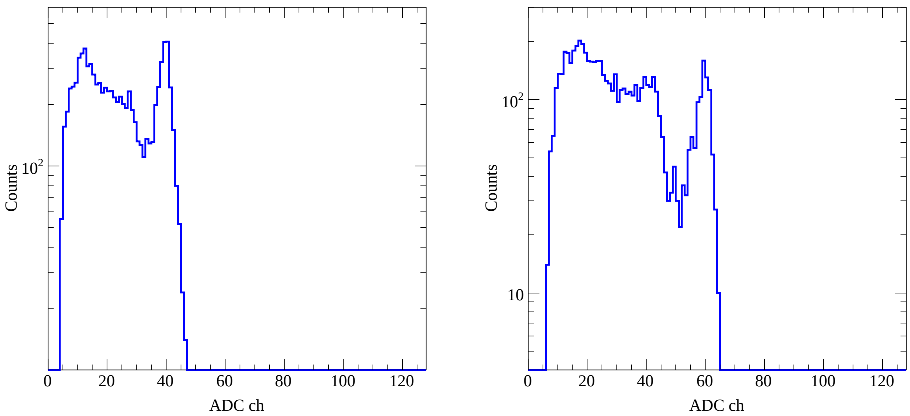

Figure 7. Example energy spectra for Ce:LYSO (*Left*) and Ce:GAGG (*Right*) matrices, extracted from the red square in figure 6.

from the MPPC arrays coincidence were within the time-window of 20 ns and their energies were within the energy-window of 511 ± 102.2 keV, the HIT address, timing and valid flag are stored in a memory for use in creating list-mode data.

In a performance test, a ^{22}Na source (0.593 MBq at the measurement date) was placed between the two detector blocks. The ^{22}Na source was contained within the central 0.25 mm ϕ region and could hence be regarded as a point source.

3.2 Result

Figure 6 show flood image results obtained for 15×15 Ce:LYSO and Ce:GAGG scintillator matrices individually coupled to the MPPC array and illuminated with a ^{137}Cs source. Figure 7 show example energy spectra extracted from the flood images. The energy resolutions for 662 keV, which were not corrected for non-linearity, were 14.0% and 9.4% for Ce:LYSO and Ce:GAGG, respectively.

Figure 8 shows the signal corresponding to 511 keV photoelectric absorption by the Ce:LYSO and Ce:GAGG. The decay time of the signals, which includes the scintillator decay time and the

2013 JINST 8 P05022

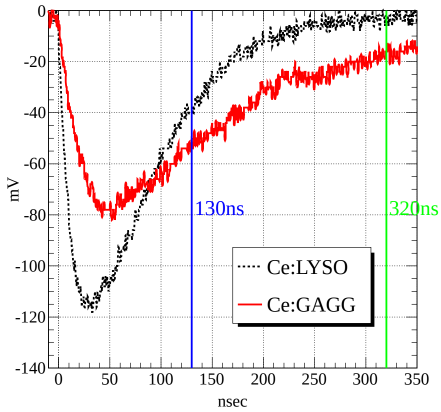

Figure 8. Signals of the Ce:LYSO and the Ce:GAGG scintillator, corresponding to 511 keV photoelectric absorption event. Red line and dashed black line represent the Ce:GAGG and Ce:LYSO, respectively.

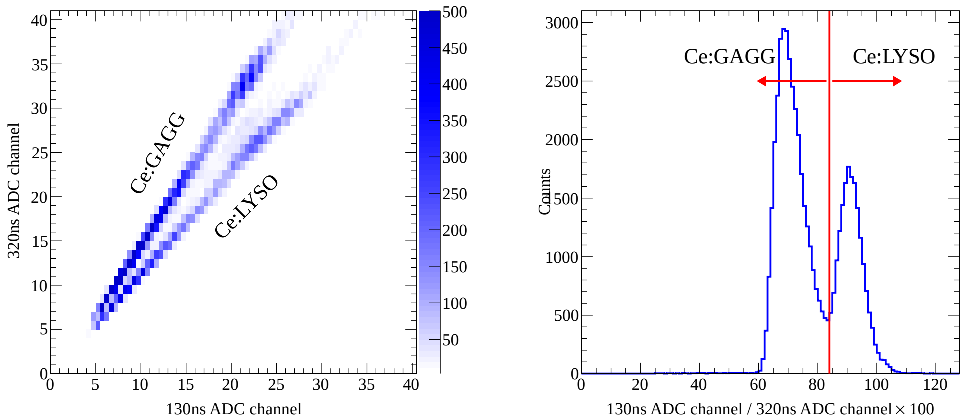

Figure 9. *Left*: 2D energy plot. x and y axis represent the 130 ns and 320 ns ADC channel, respectively. *Right*: 130 ns to 320 ns ADC channel ratio. Right peak and left peak represent the Ce:GAGG and Ce:LYSO events, respectively.

MPPC response, are approximately 70 ns and 150 ns for the Ce:LYSO and the Ce:GAGG, respectively. Figure 9 ($left$) shows the 2D energy plot; x-axis and y-axis correspond to the 130 ns and 320 ns ADC channel, respectively. For the 130 ns integration time, the signals of the Ce:LYSO is same or a little bit larger than that of Ce:GAGG as shown in figure 8, while, for the 320 ns integration time, the signals of the Ce:GAGG is larger. As a result, the events of each scintillator can be mostly separated in 2D energy plot. Figure 9 (*right*) show the 130 ns to 320 ns ADC channel ratio. If the Fast(130 ns)/Slow(320 ns) ratio is over 0.84, the event is regarded as as originating from the Ce:LYSO, and conversely if the Fast/Slow ratio is under 0.84, the event is regarded as a Ce:GAGG event. Figure 10 show the energy spectra after event selection, and each scintillator event can be effectively distinguished.

Figure 11 shows the sinogram produced by the list mode data. The two interaction positions in each coincidence event, which define the Lines of Response (LoR), were randomly determined according to the uniform distribution within the hit pixels. A simple backprojection [19] was per-

2013 JINST 8 P05022

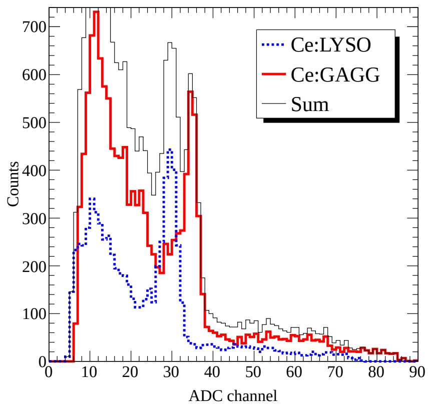

Figure 10. Energy spectra distinguished from 2D energy plot. Black line, bold red line and dashed bold blue line represent the sum, Ce:GAGG and Ce:LYSO spectra, respectively.

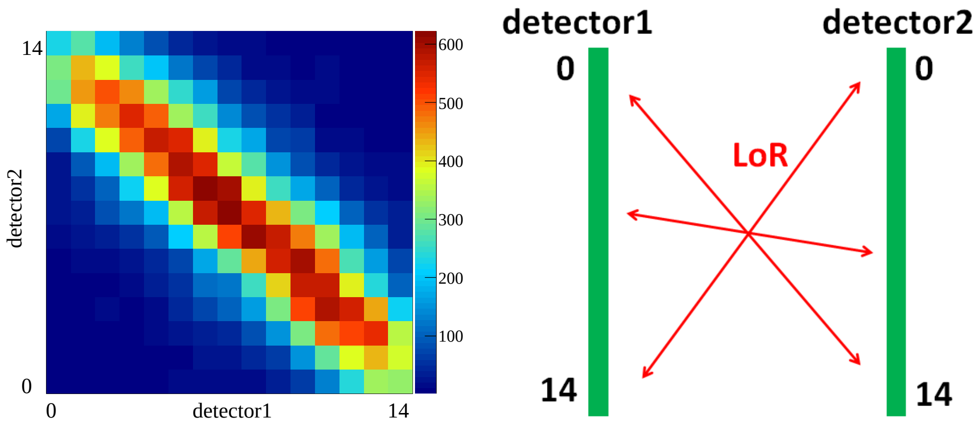

Figure 11. *Left*: coincidence diagram constructed between two detector blocks. *Right*: schematic of the backprojection process in plane view.

formed with the intersection of the all LoRs at the plane centrally located between the two detectors. Figure 12 shows the planar image of the ^{22}Na point source. The non-DoI image were reconstructed assuming that the Ce:LYSO and the Ce:GAGG pixels were a single pixel. When the DoI information was applied, the spatial resolution were 1.1 mm (x direction) and 1.4 mm (y direction), which was slightly better than the case of non-DoI (1.2mm (x direction) and 1.5 mm (y direction)).

4 Prototype gantry for a PET scanner

4.1 Setup

We plan to fabricate a PET scanner using the MPPC arrays and the fine scintillator matrices. In a preliminary performance test, two MPPC-based PET detectors consisting of the MPPC arrays, 0.5×0.5 mm^2 Ce:LYSO and Ce:GAGG scintillator matrices described in section 3 were used. The photo of the experimental setup is provided in figure 13. The 0.25 mm ϕ ^{22}Na point source

2013 JINST 8 P05022

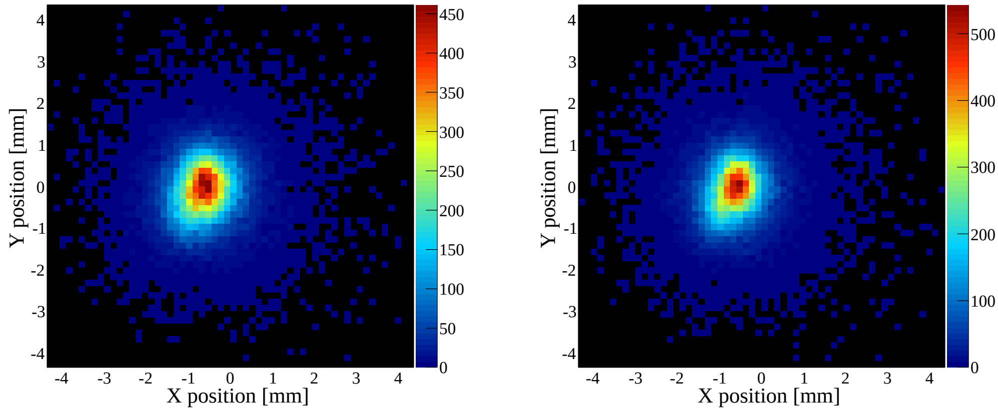

Figure 12. The reconstructed planar images applied non-DoI (*Left*) and DoI (*Right*) information.

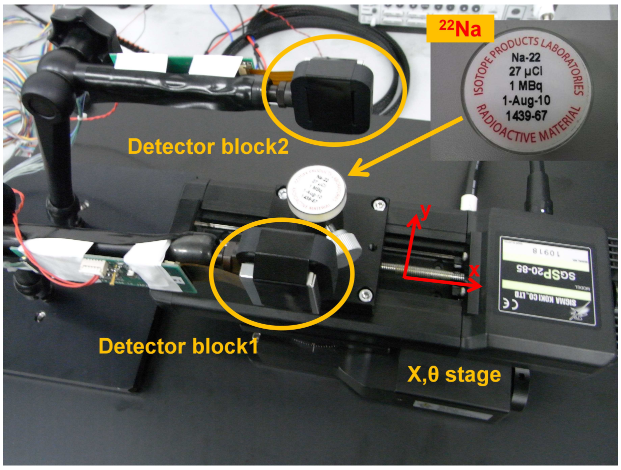

Figure 13. Experimental setup of the prototype system for a PET scanner. The distance between two detector blocks is 70 mm.

was located between the MPPC-based PET detectors, and its position was then flexibly controlled by the X-stage and the θ-stage (SGSP 80Y-AW, Sigma Koki), whose accuracy was 2.5×10^{-3} deg/pulse. Coincidence events were taken at ten source positions by changing the rotation angle (θ) at 18 degree intervals from 0 to 162 degrees. At each step, data were taken for 10 minutes.

4.2 Result

Maximum Likelihood-Expectation Maximization (MLEM) [20] method was used to reconstruct images. Figure 14 shows sinograms and the resultant reconstructed images obtained for the center and off-center (3.0 mm), respectively. The radial spatial resolution was estimated at 0.91 and 0.94 mm for the center and 3.0 mm off-center, respectively.

5 Conclusion

In this work, we have developed high spatial resolution coincidence gamma-ray cameras, which have achieved ∼1 mm spatial resolutions. The gamma-ray cameras consist of the 4×4 MPPC ar-

2013 JINST 8 P05022

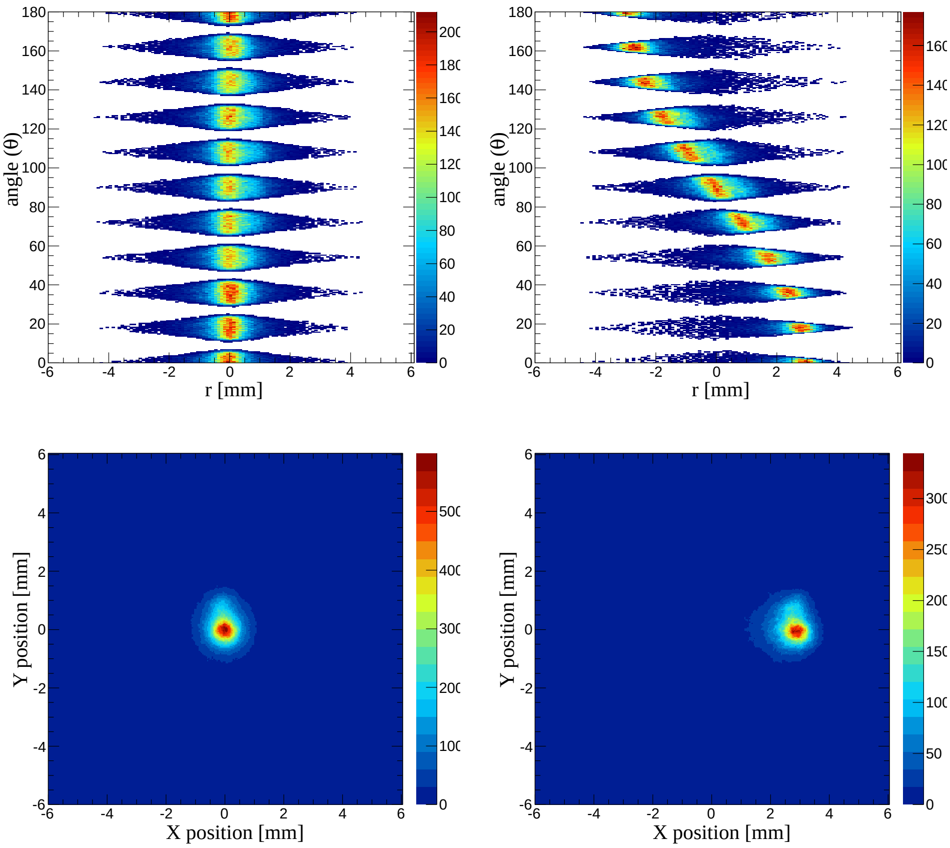

Figure 14. Sinograms and reconstructed images by MLEM algorithm, measured with a ^{22}Na point source placed at center (*Left*) and off-axis position x = 3 mm (*Right*).

rays and submillimeter pixelized scintillator matrices. The MPPC arrays have fine gain uniformity of $\pm$5.6% and very low dark count rates of $\leq$400 kcps as measured at +20 degrees. Moreover, its compactness due to the monolithic and three-side buttable structure is suited to compact medical imaging devices. The 0.5×0.5 mm^2 Ce:LYSO and Ce:GAGG scintillator matrices were used for phoswich detector. In the 2D energy plot, optical signals from the Ce:LYSO and the Ce:GAGG can be effectively distinguished. The spatial resolution of 1.1 mm was achieved for the simple planar image reconstruction when the DoI information was applied. In the preliminary measurement for a PET scanner, we used two detectors consisting of the MPPC arrays, the Ce:LYSO and the Ce:GAGG scintillator matrices with changing the rotation angle. The radial spatial resolutions of 0.91 mm (center) and 0.94 mm (3 mm off-center) were achieved from a MLEM reconstructed images. These results suggest that a monolithic MPPC array coupled with submillimeter pixelized Ce:LYSO and Ce:GAGG matrices could be promising as high spatial resolution medical imaging, and have encouraged us to develop MPPC-based modules for use in submillimeter resolution PET scanners.

Acknowledgments

We thank an anonymous referee for his/her useful comments and suggestions to improve the manuscript.

2013 JINST 8 P05022

References

[1] W.W. Moses, *Trends in PET imaging*, *Nucl. Instrum. Meth.* **A 471** (2001) 209.

[2] R.R. Raylman, et al., *Initial tests of a prototype MRI-compatible PET imager*, *Nucl. Instrum. Meth.* **A 569** (2006) 306.

[3] H. Peng et al., *Proof-of-principle study of a small animal PET/field-cycled MRI combined system using conventional PMT technology*, *Nucl. Instrum. Meth.* **A 612** (2010) 412.

[4] S. Yamamoto et al., *Design and performance from an integrated PET/MRI system for small animals*, *Ann. Nucl. Med.* **24** (2010) 89.

[5] R. Essner et al., *Application of an [^{18}F]-fluorodeoxyglucose-sensitive probe for the intraoperative detectioin of malignancy*, *J. Surg. Res.* **96** (2001) 120.

[6] E.E. Zervos,et al., *^{18}F-labeled fluorodeoxyglucose positron emission tomography-guided surgery for recurrent colorectal cancer: a feasibility study*, *J. Surg. Res.* **97** (2001) 9.

[7] S. Yamamoto et al., *Development of a positron-imaging detector with background rejection capability*, *Ann. Nucl. Med.* **20** (2006) 655.

[8] S. Yamamoto et al., *Preliminary study for the developoment of a tweezers-type coincidence detector for tumor detection*, *Nucl. Instrum. Meth.* **A 548** (2005) 564.

[9] S. Yamamoto et al., *Development of a tweezers-type coincidence imaging detector*, *Ann. Nucl. Med.* **22** (2008) 387.

[10] T. Nakamori et al., *Development of a γ-ray imager using a large area monolithic 4×4 MPPC array for a future PET scanner*, 2012 *JINST* **7** C01083.

[11] T. Kato et al., *A novel γ-ray detector with submillimeter resolution using a monolithic MPPC array with pixelized Ce:LYSO and Ce:GAGG crystals*, *Nucl. Instrum. Meth.* **A 699** (2012) 235.

[12] K. Sato et al., *Application oriented development of Multi-Pixel Photon Counter (MPPC)*, *IEEE Trans. Nucl. Sci. Conf. Rec. (NSS/MIC)* (2010) 243.

[13] I.G. Valais et al., *Evaluation of the light emission efficiency of LYSO:Ce scintillator under X-ray excitation for possible applications in medical imaging*, *Nucl. Instrum. Meth.* **A 569** (2006) 201.

[14] K. Kamada et al., 2 *inch diameter single crystal growth and scintillation properties of Ce:$Gd_3Al_2Ga_3O_{12}$*, *J. Crystal Growth* **352** (2012) 88.

[15] K. Yamamoto et al., *Development of Multi-Pixel Photon Counter (MPPC)*, *IEEE Trans. Nucl. Sci. Conf. Rec.* **N24-292** (2007) 1511.

[16] T. Kato, et al., *Development of a large-area monolithic 4×4 MPPA array for a future PET scanner employing pixelized Ce:LYSO and Pr:LuAG crystals*, *Nucl. Instrum. Meth.* **A 638** (2011) 83.

[17] S. Yamamoto et al., *Development of a high-resolution Si-PM-based γ camera system*, *Phys. Med. Biol.* **56** (2011) 7555.

[18] S. Yamamoto et al., *Development of a Si-PM-based high-resolution PET system for small animals*, *Phys. Med. Biol.* **55** (2010) 5817.

[19] P. Beltrame et al., *The AX-PET demonstrator — Design, construction and characterization*, *Nucl. Instrum. Meth.* **A 654** (2011) 546.

[20] L. Parra et al., *List-mode likelihood: EM algorithm and image quality estimation demonstrated on 2-D PET*, *IEEE Trans. Med. Imag.* **17** (1998) 228.

2013 JINST 8 P05022